10.21611/qirt.2023.22

QIRT Asia 2023

4th Asian Quantitative InfraRed Thermography Conference

Curved CFRP Specimen: Thermographic Inspection and Simulation

by S. O. A. Gnessougou*, S. Unnikrishnakurup**, A. Ngo Chun Yong**,

P. Servais***, C. Ibarra -Castanedo*, X. Maldague*

* Department of Electrical and Computer Engineering, Université Laval, 1065, av. de la Médecine, Québec, G1V 0A6, Québec, Canada
** Institute of Materials Research & Engineering (IMRE), Agency for Science, Technology and Research (A*STAR), 2 Fusionopolis Way, #08-03 Innovis, Singapore 138634
*** MPP, Aero & Industrial Solutions 1er avenue 66 – B-4040 Herstal, Belgium

INTRODUCTION

Infrared thermography is an engineering technique that allows the evaluation and characterization of materials in non-destructive ways. It finds many applications in the field of aeronautics, the environment, archaeology, art history, building inspection, certain medical tests, etc. In pulsed thermography, thanks to an external thermal source, the material to be analyzed is briefly heated. The thermal wave front propagates through this material and the existence of internal defects generates temperature gradients (with respect to areas without defects) [1, 2]. The presence of subsurface defects can be observed using an infrared camera either on the front or the rear surface. In composite materials, infrared thermography can detect relatively shallow defects (typically a few millimetres), this is due to the anisotropy that limits the propagation of the thermal wave front in depth. The images obtained by the infrared camera consist of temporal thermograms that can be further analysed by advanced signal processing techniques such as pulsed phase thermography (PPT) [3], from which frequency phasegrams can be produced. Temporal thermograms are greatly affected by the structure of the material, surrounding reflections and emissivity variations. Frequency phasegrams on the other hand, are less affected by these constraints and allow fault detection up to twice the depth of the temporal thermogram.

In this project the inspection of curved composite materials by pulsed thermography is investigated. Non-planar components pose special challenges due to their geometry. An example of such specimen is shown on Fig. 1.

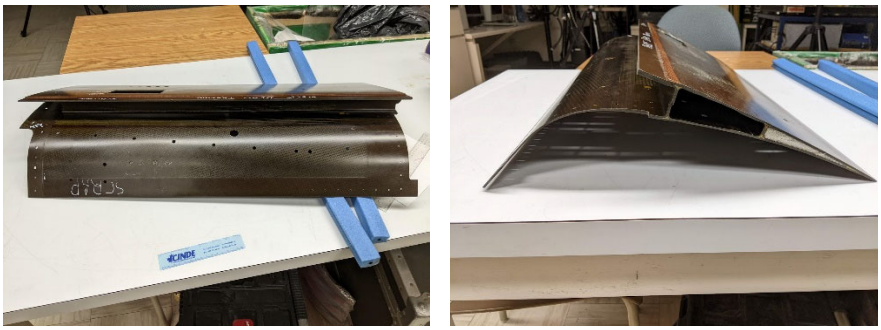

Figure 1: Example of curved composite specimen used in this study.

1. EXPERIMENTAL SET-UP

A high-definition cooled IR camera (FLIR X8501sc, NETD < 20 mK, InSb, 3-5 µm, 1280 x 1024 pixels, linear Sterling cooling, lens focal length = 17 mm) and two Xenon flashes (Balcar, 6.2 kJ per flash,

pulse duration 2 ms @ FWHM) were used and synchronized through a PC. The specimen shown in Figure 1) was inspected in reflection mode as depicted in Figure 2. The camera was positioned at approximately 80 - 100 cm from the specimen while the flashes were placed at a distance of 25 cm from the front side of the specimen forming a 45˚ angle with respect to the specimen surface. Thermographic sequences of 1000 frames at 40 fps were collected and processed.

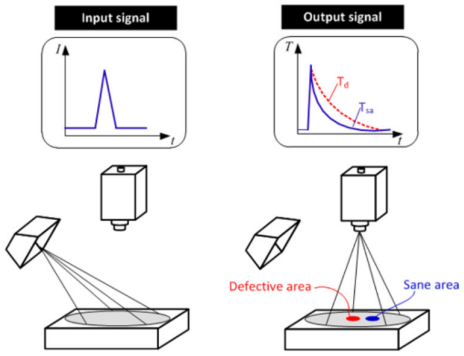

Figure 2 : Schematic of the experimental apparatus

2. EXPERIMENTAL RESULTS AND ANALYSIS

The sample contains 6 flat-bottom-holes (FBH) with the dimensions and depths indicated in Table 1. ir-view software (Visiooimage inc.) was used to produce the graphics and process data. Figure 3 shows screen shots (arbitrarily chosen) of a phasegram (left) and a thermogram (right) as examples. Figure 4 presents the thermal profiles (temperature evolution through time) of a sound area compared to the three FBHs and the corresponding thermal contrast profiles. As can be seen from these graphs, the thermal profile of the shallowest defect shows the highest temperature, which reduces as the defect depth increases. The thermal contrast profiles are calculated as the arithmetic difference between the thermal profiles of each defect and the thermal profile of the sound area. As can be seen, the thermal contrast profiles show a maximum that is related to the defect depth: for shallow defects it occurs earlier and with greater contrast than for deep defects.

Frequency thermograms have also better contrasts compared to temporal thermograms. For the first series of the three diameter defects D1, D2, D3) and at the three different depths (Dp1, Dp2, Dp3), the contrasts of the temporal and frequency thermograms reveal clearly observe the defects (Figs. 4, 5).

Set of defects (type FBH – Flat Bottom Holes) have the following dimensions:

FBH	Dimensions	
	Diameter in(mm)	Depth in(mm)
D1	2.49(63.246)	0.38(9.652)
D2	2.49(63.246)	0.44(11.176)
D3	2.47(62.738)	0.56(14.224)
D4	3.72(94.488)	0.26(6.604)
D5	3.71(94.234)	0.41(10.414)
D6	3.71(94.234)	0.54(13.716)

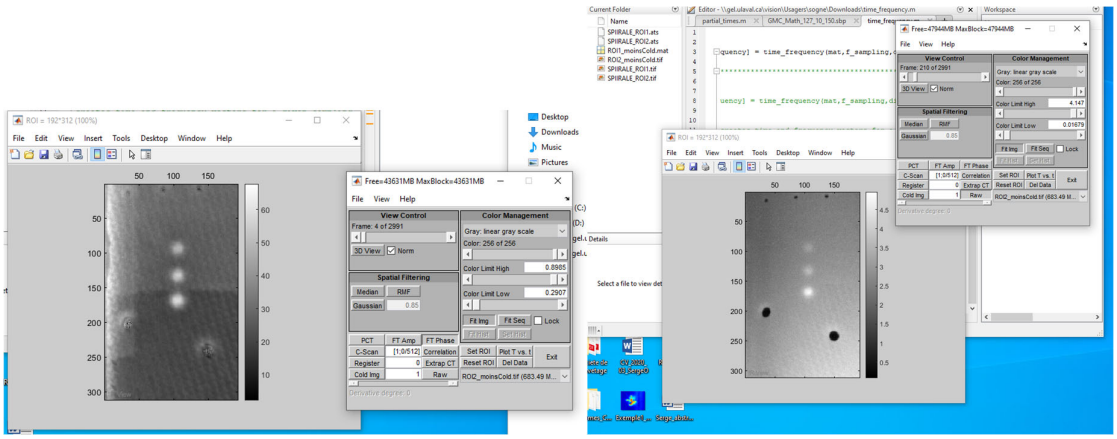

Figure 3 : First set. Examples of phasegram (left) and thermogram (right).

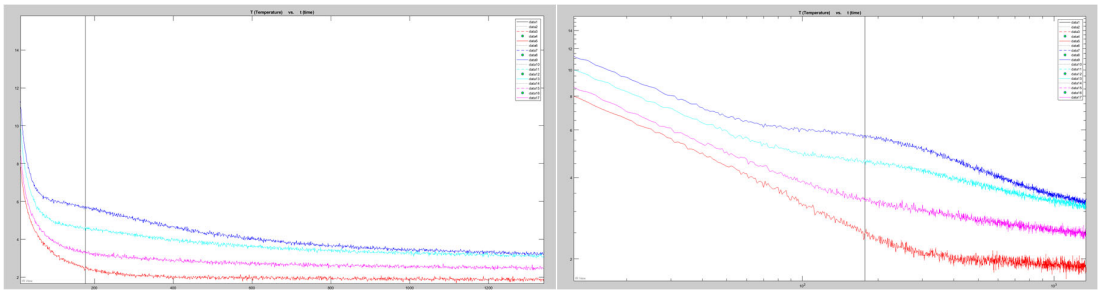

not Log scale for time in x axis Log scale for time in x axis

Figure 4: First set. Temperature temporal evolution for the 3 FBHs, red is the sound area reference.

For the second set of defects (D4,D5,D6), the contrasts of the frequency thermograms allow also to clearly observe the three defects, independently of the depth (Dp4,Dp5, Dp6). For the temporal thermograms, thermal contrast helps to visualize the first two depths (Dp5, Dp6) and not the third depth (Dp6), Fig. 5, 6.

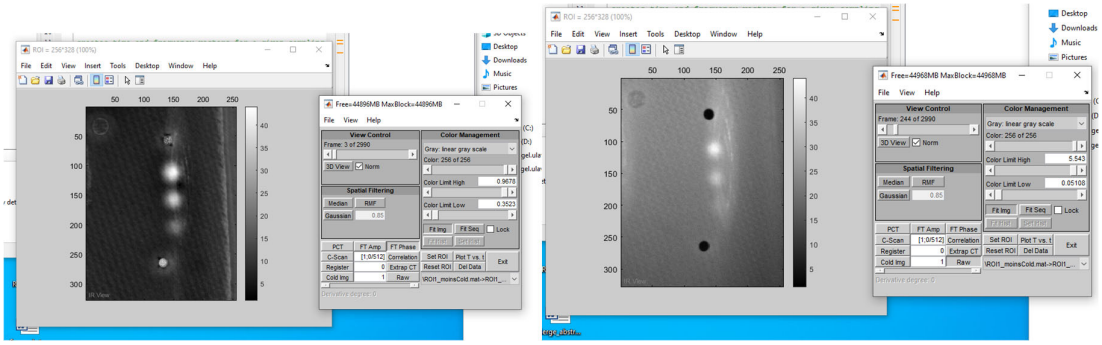

Frequential thermogram Temporal thermogram

Figure 5 : Second set. Examples of phasegram (left) and thermogram (right).

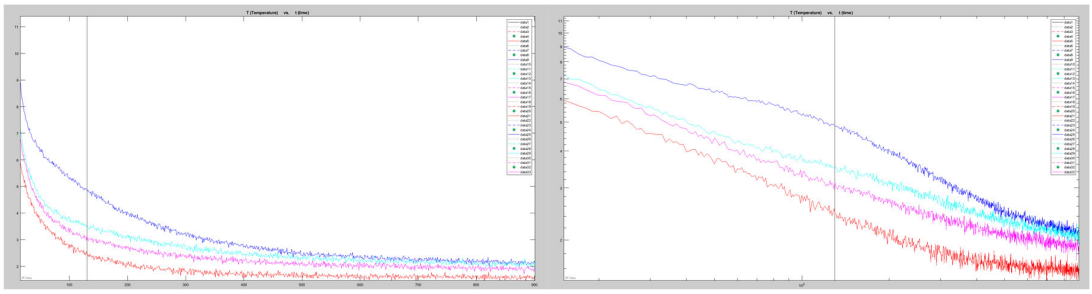

Not Log scale for time in x axis Log scale for time in x axis

Figure 6: Second set. Temperature temporal evolution for the 3 FBHs, red is the sound area reference.

Interestingly the two defect sets (1, 2) were on the curved part. We also tested FBHs on the flat side in the same conditions, this time with the defects are perpendicular to the camera optical axis. We noted an increase for the thermal contrast clearly confirming the effect of the curvature on the measurements, this was expected as used in fact in 'shape from heating' approach [4]. However, the curvature of the specimens had no effect on the phase ø images due to the ratio involved in the computations [1]:

$$A_n = \sqrt{\mathrm{Re}_n^2 + \mathrm{Im}_n^2} \quad \text{and} \quad \phi_n = a\tan\frac{\mathrm{Im}_n}{\mathrm{Re}_n} \tag{1}$$

where Re and Im are respectively the real and imaginary parts of the Fourier decomposition in PPT, A is the amplitude (contrast).

3. Simulations

We also simulated the specimens using commercial software COMSOL Multiphysics with the following parameters, surface heat flux and specimen geometry (matching s much as possible the real specimen):

Material	Thickness in mm	K(W/mK)	Density (kg/m3)	Specific heat (J/kgK)	Diffusivity x10^{-6} m^2/s
CFRP	15	{7, 4, 0.7}	1600	1200	0.37±0.02

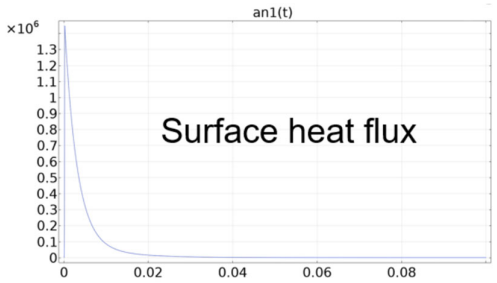

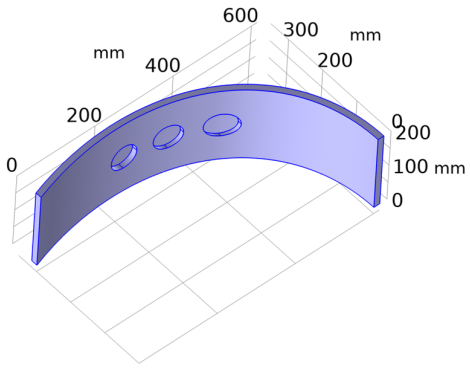

The following images present the simulation's results:

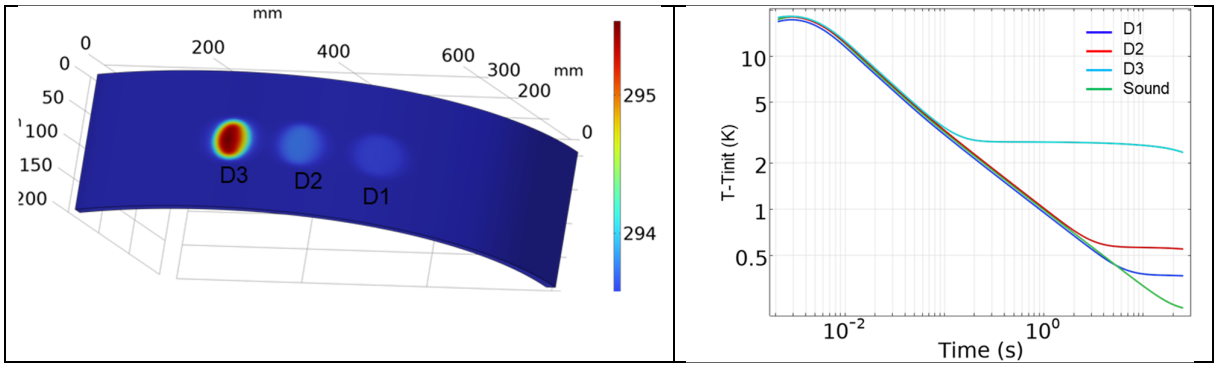

4. Discussion and conclusion

In this study, we tested and simulated the thermal behavior of a typical CFRP specimen with several FBHs in both flat and curved areas. The same specimens were modelled as well using COMSOL. In both cases, we noticed, as expected, that temporal contrast images, i.e. the thermograms, are affected by the curvature of the specimens. On the contrary, phasegrams resulting from pulsed phase thermography processing are not affected by the specimens' geometry.

Although simulations and experiments cannot be directly compared at this point of our investigation, all the artificial defects could be detected in both experiments and simulations. Further analysis is underway to better understand the similarities and differences between experiments and simulations.

Acknowledgement

This work was supported by the Natural Sciences and Engineering Research Council (NSERC) Canada through the Discovery and CREATE 'oN DuTy!' program as well as the Canada Research Chair in Multipolar Infrared Vision (MiViM). This work is also supported by the Agency for Science, Technology and Research (A*STAR) through grants under its Singapore Aerospace Programme cycle 15 (Grant No. M2115a0093) and AISG grant SC25/22-722917.

We acknowledge the contribution of Ministère des Relations internationales et de la Francophonie of Quebec in the framework of the Quebec/Singapore scientific collaboration, project SPiiRALE.

References

[1] X. Maldague, *Theory and Practice of Infrared Technology for NonDestructive Testing*, John Wiley & Sons, New York, 684 p., 2001.
[2] consult www.qirt.org archive website for numerous pertinent papers.
[3] X. Maldague, S. Marinetti, "Pulse Phase Infrared Thermography," *J. Appl. Phys.*, 79[5]: 2694-2698, 1996.
[4] J.-F. Pelletier, X. Maldague, "Shape from Heating: A Two-Dimensional Approach for Shape Extraction in Infrared Images, " *Optical Engineering*, **36**[2]: 371-375, Feb. 1997.